



Preparation and analysis of biodegradable polydioxanone/chitosan film

Ji Yun Nam¹ · Young Seok Song¹

Received: 9 December 2021 / Accepted: 11 May 2022 / Published online: 18 May 2022
© The Polymer Society, Taipei 2022

Abstract

In this study, we investigated the miscibility and degradability of biodegradable polymers. Polydioxanone (PDO) was blended with chitosan, and the resulting films were prepared via film casting. The blends were analyzed according to composition ratio and in vitro biodegradation. The intermolecular interaction in the blend was verified through spectroscopic analysis. The addition of chitosan was found to lead to a significant enhancement in the mechanical properties of the blend. Also, the chitosan embedded film showed different morphologies and thermal properties from the pure PDO film. The current study might show a possibility of employing PDO based biodegradable film for biomedical applications.

Keywords Polydioxanone (PDO) · Chitosan · Miscibility · Biodegradability

Introduction

GBR(guided bone regeneration) is a surgical procedure that helps bone formation by using a barrier membrane when there is a lack of bone around the implant assembly [1, 2]. Also, It is important to prevent the faster formation of dental epithelium than bone [3]. The barrier membrane is divided into two main types depending on its absorbency: Non-absorbable membrane such as e-PTFE (expanded-polytetrafluoroethylene) is widely used but requires the secondary removal surgical procedure. On the other hand, since absorbable membrane such as collagen does not need additional surgery, infection risk is relatively low [4]. However, the absorbable membrane has quite low mechanical properties to maintain dimensional stability [5–7]. It is necessary to increase its strength to prevent tearing during surgical procedure.

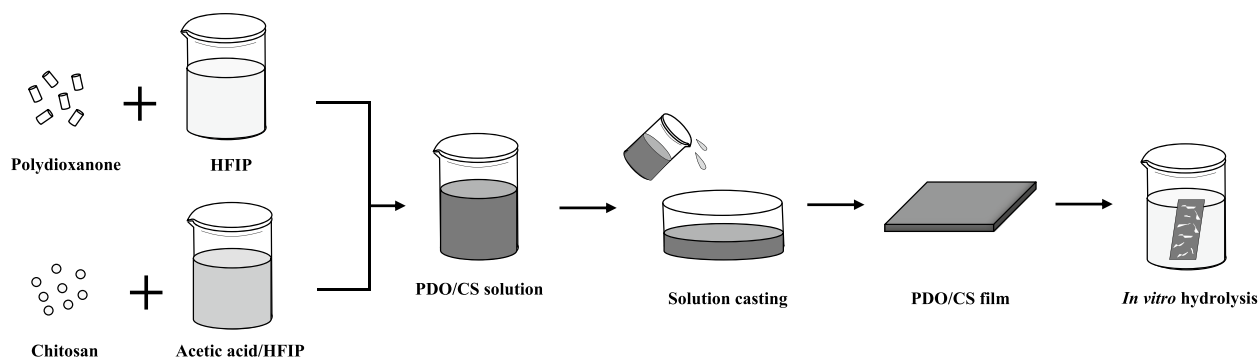
Biodegradable polyesters such as polylactic acid (PLA), polycaprolactone (PCL), polyglycolic acid (PGA), polyhydroxy butyrate (PHB) and polydioxanone (PDO) attract a lot of attention in the medical industry [8, 9]. For instance, PDO has excellent biodegradability and biocompatibility. However, its commercial applications are limited due to high cost

and low strength. Thus far, a few studies have been done on the characteristics of PDO, especially biodegradability. Sabino et al. introduced the hydrolysis process of PDO and showed biodegradable behavior in PBS solution [10]. Some attempts have been made to improve the physical properties of PDO and control the degradation behavior. Bai et al. incorporated PPDO with PDLLA by the film casting and analyzed the hydrolysis behavior according to the blend composition [11]. Also, Ebrahimpour et al. investigated the miscibility of biodegradable PBS and PDO by using a viscometer [12]. The blending method enables one to control the biodegradation of polymer as well as to improve physical properties of components [13]. Chitosan is derived by deacetylation of chitin, which is easy to obtain from crabs, lobsters, and shrimps [14, 15]. Since chitosan has biodegradable, biocompatible, nontoxic, and relatively good mechanical properties among other natural materials, it has been applied to biodegradable blends [16, 17]. Since chitosan can form the intermolecular interaction with other polymers due to the amino and hydroxyl groups, they have been used as a blending material to optimize physicochemical properties of polymeric parts [18].

In the current study, biodegradable PDO/chitosan films were manufactured using the film casting, and their mechanical, thermal and chemical properties were evaluated. In addition, the chemical characteristics of the blend was analyzed using fourier transform infrared (FT-IR) and nuclear magnetic resonance (NMR) spectroscopy. The biodegradability test was conducted for 12 weeks.

✉ Young Seok Song
ysong@dankook.ac.kr

¹ Department of Fiber Convergence Materials Engineering,
Dankook University, Gyeonggi Do 16890, Republic of Korea



Scheme 1 Schematic illustration of preparation of the PDO/chitosan (CS) films

Experimental

Materials

PDO (DO-013) was purchased from Meta-Biomed Co. (Korea). It has a melt flow index of 2 at 170 °C. Chitosan supplied by Aldrich has a viscosity of 20–300cP in the acetic acid solution and a degree of deacetylation > 75%. 1,1,1,3,3,3-Hexafluoro-2-propanol (HFIP, > 99%) and acetic acid (> 99.5%) were provided by TGI (Tokyo, Japan) and SAMCHUN pure chemical Co. (Korea), respectively. Phosphate-Buffered Saline (PBS, 7.38 pH) was purchased from BIONEER (Korea).

Film preparation

PDO and chitosan were blended via the film casting method (Scheme 1). First, PDO was dissolved in HFIP of 1% w/v concentration at 60 °C for 2 h, and then chitosan was dissolved in acetic acid-HFIP (1:15 v/v) at room temperature. The two solutions were mixed with a magnetic stirrer. The mixed solution was poured into a glass mold, and the solvent was evaporated at 60 °C for 3 days under vacuum. The blend films (PDO/chitosan) were prepared according to the following composition: 100/0, 90/10, 80/20, and 70/30 w/w.

Fig. 1 FTIR spectra of the PDO/chitosan films: **a** 100/0, **b** 70/30, and **c** 0/100 ratios

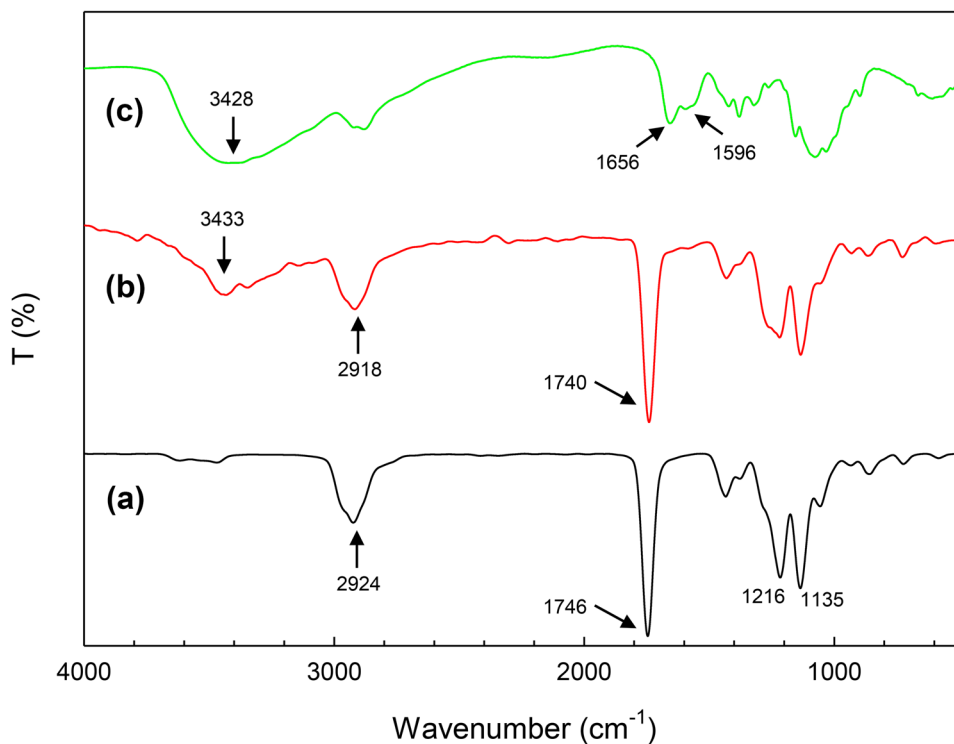
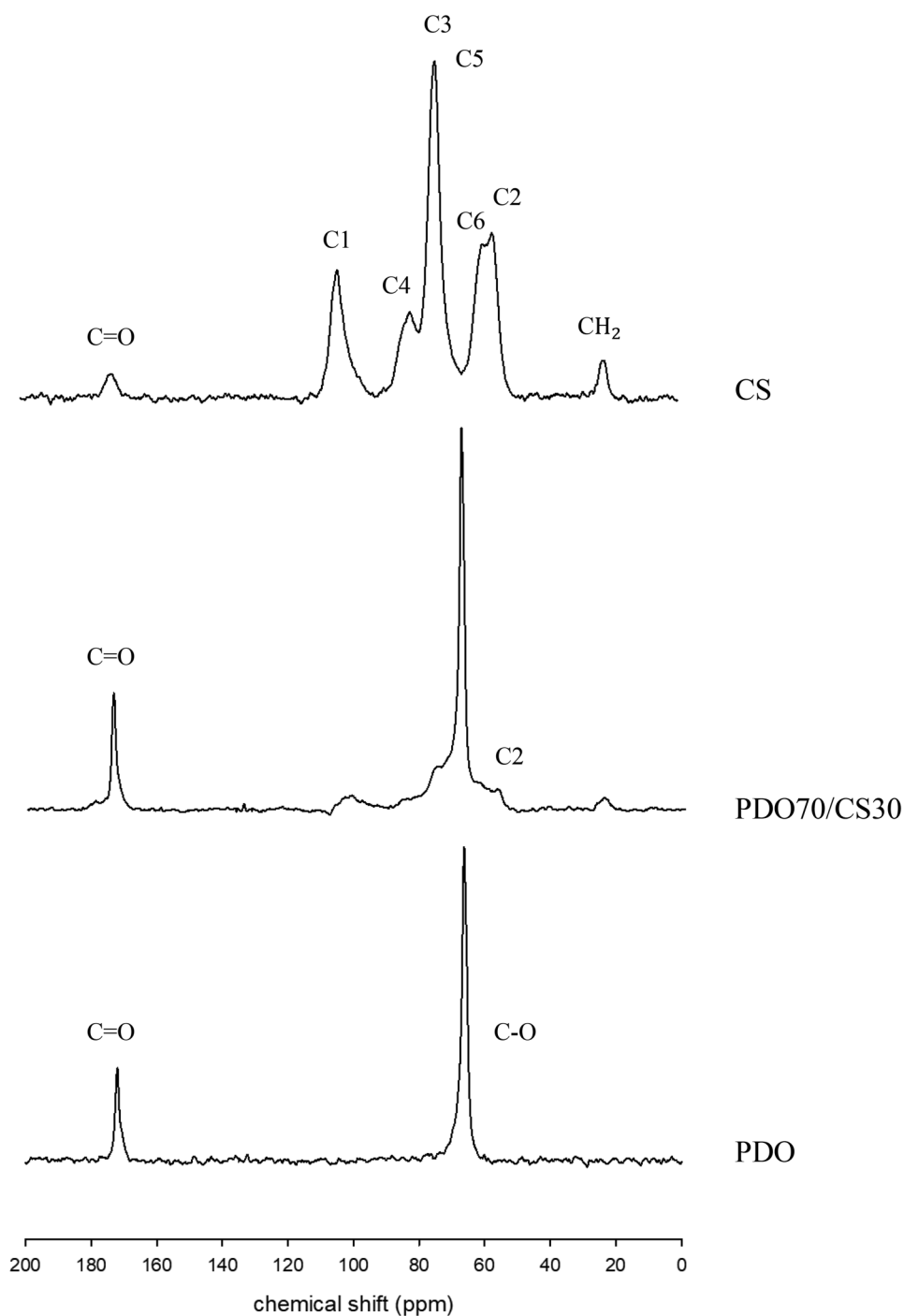


Fig. 2 CP/MAS ^{13}C NMR spectra of the chitosan, PDO/chitosan (CS), and PDO films



Film characterization

The prepared specimens were used to measure mechanical properties such as tensile strength, Young's modulus and elongation at break at an extension speed of 5 mm/min with a universal testing machine (UTM, Instron). Dynamic mechanical analysis (DMA) was carried out to characterize the viscoelastic properties such as storage modulus and loss modulus while applying a frequency sweep of 0.01-100 Hz.

Prior to the test, a pre-tension process was applied. The measurements were conducted using a rheometer (MCR302 Anton-Paar) with a UXF kit. Thermogravimetric analysis (TGA) of the blend films was carried out with a thermogravimetric analyzer (TGA N-1000, Scinco). The samples were heated from room temperature to 600 °C at a heating rate of 10 °C/min under a nitrogen flow of 100 mL/min. To confirm the intermolecular interaction in the blend, the film was scanned between 400 cm^{-1} and 4000 cm^{-1} using

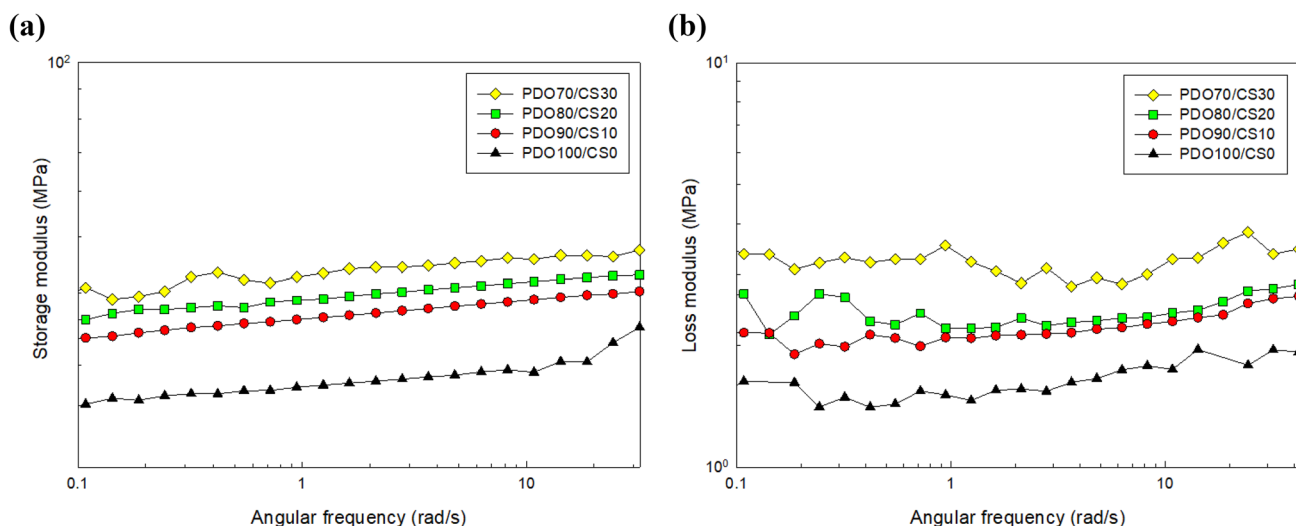


Fig. 3 **a** Storage modulus (E') and **b** loss modulus (E'') of the PDO/chitosan films as a function of the angular frequency

an FT-IR spectrometer (Spectrum Two, PerkinElmer). Also, a 500 MHz solid-state ^{13}C NMR spectra were obtained at room temperature by using a Bruker Avance II spectrometer at room temperature. The CP/MAS mode was employed for all samples using a 4 mm probe. A spinning speed of 5 kHz and a pulse repetition delay of 5 s were used.

In vitro degradation

For the in vitro degradation, The PDO/chitosan blend films were immersed in phosphate buffer solution (PBS). Degradation test was carried out in an incubator at 37 °C for periods 12 weeks. For the test, the specimens were washed with distilled water to remove the hydrolysis medium and

dried in a vacuum oven at room temperature. The films were placed in a desiccator before the measurement. To analyze hydrolysis, the change in pH was measured with a pH meter (Model 700, EUTECH). The residue weight was calculated according to the following formula:

$$\text{Residue weight (\%)} = \frac{W_r}{W_0} \times 100\% \quad (1)$$

where W_0 and W_r are the initial and residual weights of the specimens, respectively. The morphological characteristics of the samples were analyzed according to the degree of degradability by using scanning electron microscopy (SEM, S-4700 Hitachi). The thermal properties of the samples were probed using a differential scanning calorimeter (DSC4000,

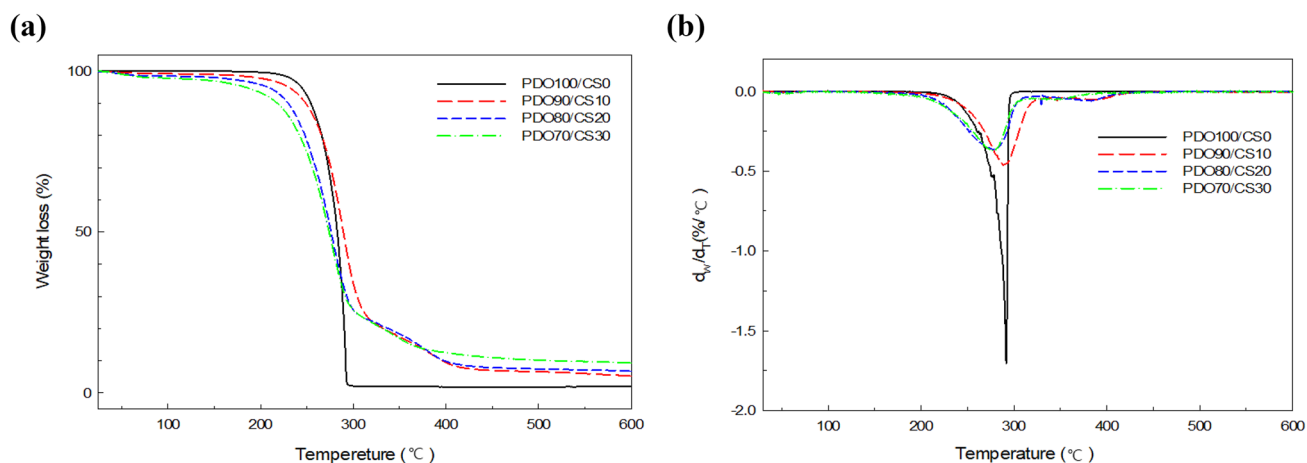
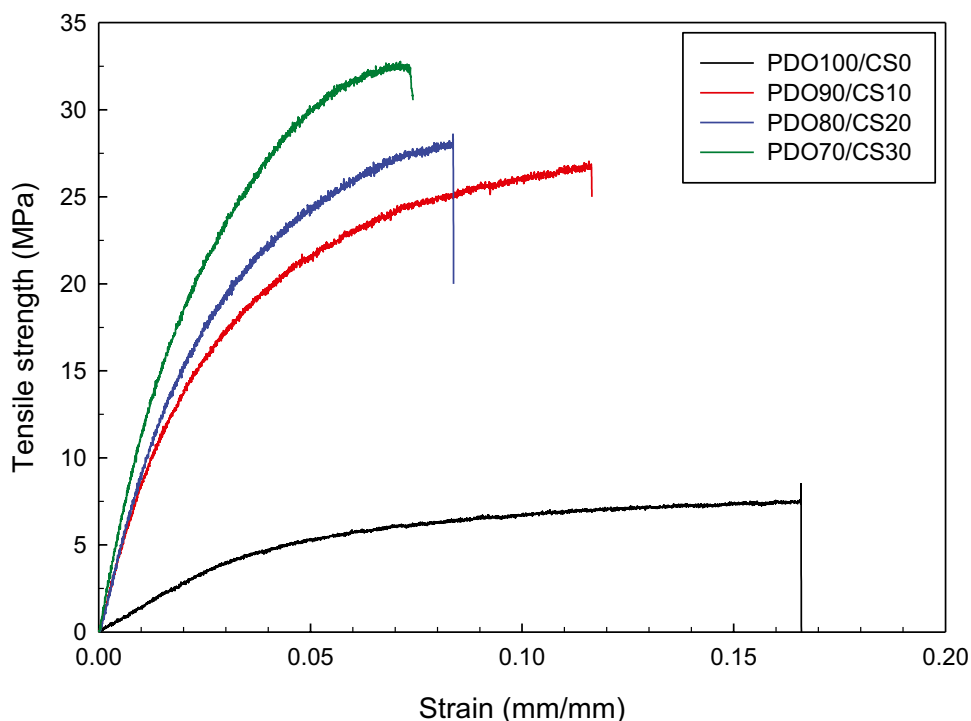


Fig. 4 **a** TGA result and **b** DTG result of the PDO/chitosan films as a function of the temperature

Fig. 5 Stress–strain curves of the PDO/chitosan films

Perkin Elmer). The samples were heated from an ambient temperature to 150 °C at a heating rate of 10 °C/min. The exothermic and endothermic peaks were ascribed to the melting point (T_m) and the crystallization temperature (T_c) in the second heating step, respectively. The following equation was employed to obtain the crystallinity of the blend films.

$$Dc_{blend}(\%) = \frac{\Delta H_m}{\Delta H_m^0} \times 100 \quad (2)$$

$$Dc_{pdo}(\%) = \frac{Dc_{blend}}{W_{pdo}} \quad (3)$$

$$W_{pdo}(w/w) = \frac{PDO}{PDO + CS} \quad (4)$$

where ΔH_m is the enthalpy of melting per gram of blend, W_{pdo} is the weight fraction of PDO in the blend, and ΔH_m^0 is the enthalpy of melting for 100% crystalline PDO [19].

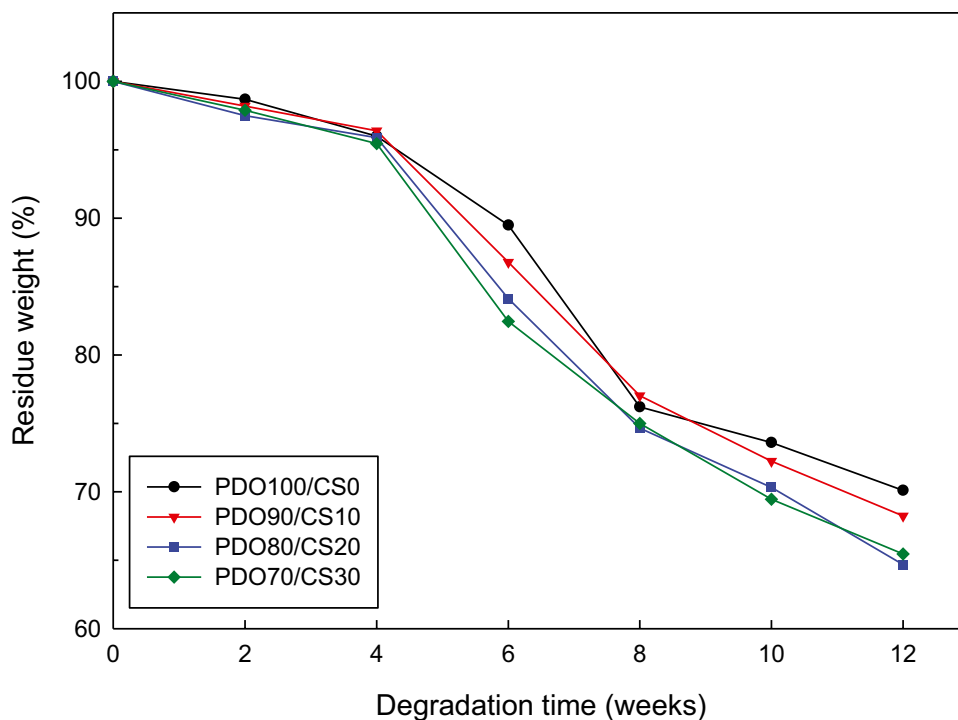
Results and discussion

Figure 1 shows the FTIR spectra of the prepared PDO/chitosan films with blend ratios of 100/0, 70/30, and 0/100. The characteristic peaks of chitosan were observed at 3428 cm^{-1} , which implies $-NH_2$ and $-OH$ groups stretching vibration. The peaks at 1656 cm^{-1} and 1596 cm^{-1} indicate the $CONH_2$ and NH_2 groups, respectively [20]. For the PDO film, the strong and sharp absorption bands at 2924 cm^{-1} and 1746 cm^{-1} are assigned to the C-H and C=O stretching vibration, respectively. The peaks at 1216 cm^{-1} and 1135 cm^{-1} are ascribed to the C–O–C stretching vibration. In addition, the small peak around 3472 cm^{-1} was observed, indicating the existence of the end O–H from macromolecular chains [12]. For the PDO/chitosan film with a blend ratio of 70/30, similar results were obtained, which supports the existence of PDO and chitosan in the blend film. On the other hand, frequency shifts show a specific interaction between the characteristic groups of

Table 1 Mechanical properties of the PDO/chitosan films

	Young's Modulus (MPa)	Tensile Strength (MPa)	Strain at break (mm/mm)	Elongation at break (%)
PDO100/CS0	140.91	7.75	0.17	22.40
PDO90/CS10	834.64	27.03	0.12	17.46
PDO80/CS20	904.59	28.22	0.08	12.55
PDO70/CS30	1108.42	32.75	0.07	11.12

Fig. 6 Residue weight of the PDO/chitosan blend films with respect to the degradation time

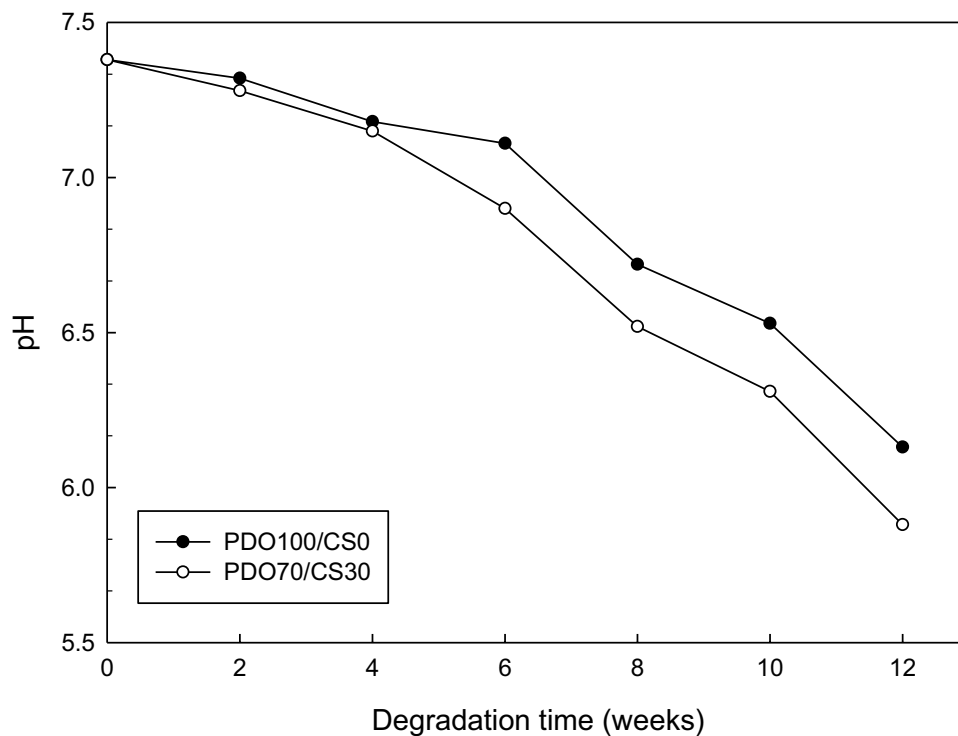


the pure polymers [21]. The peak of stretching vibration of carbonyl in PDO (1746 cm^{-1}) was shifted to lower wave number (1740 cm^{-1}) after blending with chitosan due to the formation of intermolecular hydrogen bonds between PDO and chitosan [22]. Also, the spectrum of PDO/chitosan film shows the shifts from 3428 to 3433 cm^{-1} was

observed for the stretching vibration of $-\text{NH}_2$ and $-\text{OH}$ groups.

In order to further investigate the intermolecular interactions of the blend, the CP/MAS ^{13}C NMR spectra of the chitosan, PDO, PDO/chitosan films were obtained as shown in Fig. 2. The peaks of the $\text{C}=\text{O}$ and $\text{C}-\text{O}$ units of

Fig. 7 pH change of the buffer solution with respect to the degradation time



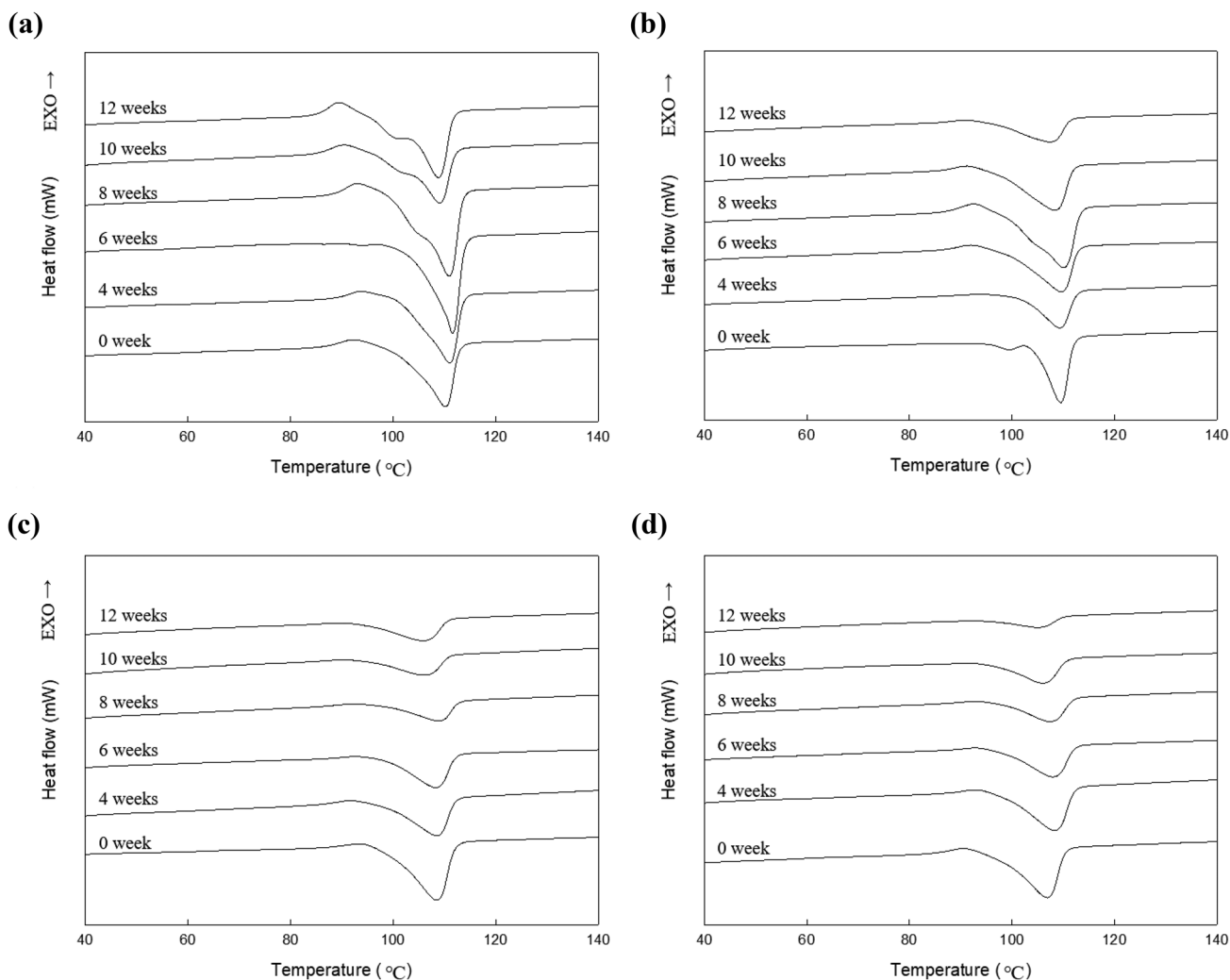


Fig. 8 DSC results of the PDO/chitosan blends with respect to the degradation time: **a** 100/0, **b** 90/10, **c** 80/20, and **d** 70/30 ratios

PDO appeared at 172 and 66.25 ppm, respectively. In the case of the pure chitosan, the residual acetyl group appeared at 172.36 ppm, while the residual methyl group was determined at 22.62 ppm [23]. It is known that the amino units linked to the C2 atoms of chitosan can form intermolecular hydrogen bonds with the carbonyls units [24, 25]. This interaction affects the electron density around the carbons, which causes the changes in chemical shifts [26]. The C2 resonance peak of the PDO/chitosan at $\delta = 56.91$ ppm shows downfield shifts. From the results from FTIR spectra and solid-state ^{13}C NMR spectra, the existence of the intermolecular hydrogen bonds between CS and PDO was confirmed.

DMA tests can help ones to understand the long-term stability of the dispersion and the behavior of the polymer. Figure 3 shows the storage modulus (E') and loss modulus (E'') of the PDO/chitosan film as a function of

angular frequency. All the specimens showed that E' was higher than E'' , which indicates a dominant elastic solid-like behavior [27]. Both the storage and loss modulus increased as a function of angular frequency. Additionally, the modulus values of the film blended with chitosan had higher than the pure PDO. This is because of the relatively large elastic feature of chitosan [28]. These results were similar to the tensile test results of the PDO/chitosan blend film.

The thermal behavior of the PDO/chitosan blend film is demonstrated in Fig. 4. The initial degradation temperature of PDO film was 220 °C, and the decomposition temperature was found around 290 °C. There are two degradation steps in chitosan [29]. For the case with a weight ratio of 70:30, the weight loss firstly started at 200 °C and became around 75% at 300 °C. The maximum weight reduction rate

Table 2 Thermal properties of the PDO/chitosan films

	PDO100/CS0				PDO90/CS10				PDO80/CS20				PDO70/CS30			
	T_m (°C)	ΔH_m (J/g)	$D_{C_{blend}}$ (%)	$D_{C_{pdo}}$ (%)	T_m (°C)	ΔH_m (J/g)	$D_{C_{blend}}$ (%)	$D_{C_{pdo}}$ (%)	T_m (°C)	ΔH_m (J/g)	$D_{C_{blend}}$ (%)	$D_{C_{pdo}}$ (%)	T_m (°C)	ΔH_m (J/g)	$D_{C_{blend}}$ (%)	$D_{C_{pdo}}$ (%)
0 weeks	110.3	66.1	46.8	46.8	109.5	51.9	36.8	40.9	108.7	51.1	36.2	45.3	107.0	50.1	35.5	50.7
4 weeks	111.0	70.0	49.6	49.6	109.3	44.2	31.3	34.8	108.5	37.1	26.3	32.9	108.3	40.5	28.7	41.0
6 weeks	111.7	67.6	47.9	47.9	109.7	49.8	35.3	39.2	108.3	34.4	24.4	30.5	108.0	34.1	24.2	34.6
8 weeks	111.0	75.1	53.2	53.2	110.2	65.8	46.6	51.8	109.0	31.0	22.0	27.5	107.5	31.5	22.3	31.9
10 weeks	109.2	67.6	47.9	47.9	108.5	54.5	38.6	42.9	106.0	30.6	21.7	27.1	106.0	28.8	20.4	29.1
12 weeks	109.0	62.2	44.1	44.1	107.5	42.6	30.2	33.6	106.0	29.6	21.0	26.3	105.5	17.5	12.4	17.7

occurred at 280 °C. Secondly, the specimen showed 85% weight reduction at 360 °C. In the case of the blend films, as the content of the chitosan increased, the degradation temperature decreased. The total weight losses of 90/10, 80/20, and 70/30 at 600 °C were found to be 94.7%, 93.2%, and 90.7%, respectively.

Mechanical strength is important for medical applications. Currently, the usage of PDO film is quite limited due to its low strength [30]. Mechanical properties including Young’s modulus, tensile strength and elongation at break were analyzed to evaluate the addition effects of chitosan to the PDO film. Figure 5 shows that the blended film had dramatically increased strength compared to the pure PDO film. Also, the tensile strength increased with increasing the chitosan content. However, the elongation at break decreased with an increase in the chitosan fraction. Since chitosan acts as a reinforcing agent, the higher content lead to the higher rigidity [31]. The decrease in the elongation at break is related to an increase in the stiffness of the blend films as a result of the addition of chitosan [32].

As listed in Table 1, the addition of chitosan plays a key role in increasing the strength of the PDO film. In the case of the blend film with a 30 wt% chitosan fraction, the tensile strength and Young’s modulus showed the highest values of 32.75 MPa and 1108 MPa, respectively. From this, it is inferred that chitosan can serve as a reinforcing phase in the blend matrix.

The percentage of residue weight for the PDO/CS blend films is demonstrated in Fig. 6. According to the hydrolysis mechanism of aliphatic polyesters such as PDO, once water penetrates into polymer it breaks the ester bond and creates short and soluble fragments of molecular chains. As a result, this results in the residue weight and decreases pH [33]. For the pure PDO film, the largest mass reduction between 6 and 8 weeks was found. This implies that the soluble fragments were produced after 6 weeks by hydrolysis. When the chitosan was added to the PDO, the residue weight was decreased. This result indicates that the presence of chitosan expedites the hydrolysis (Fig. 7). After 12 weeks of hydrolysis, the pure PDO and the blend film with 30 wt% chitosan contents showed the reductions in the pH values from 7.38 to 6.13 and 5.88, respectively.

The DSC thermograms of the PDO/chitosan films are presented in Fig. 8. The blend film showed a single melting temperature, which indicates a good miscibility of the PDO and chitosan. As the hydrolysis progressed, both the melting temperature (T_m) and enthalpy of melting (ΔH_m) increased. This result is similar to the result reported by Sabino et al. [10]. This is because the amorphous region is first attacked due to the hydrolysis, thus resulting in the scission of unstable ester chains. This led to the reduction in the chain entanglements and the increment in the crystallinity

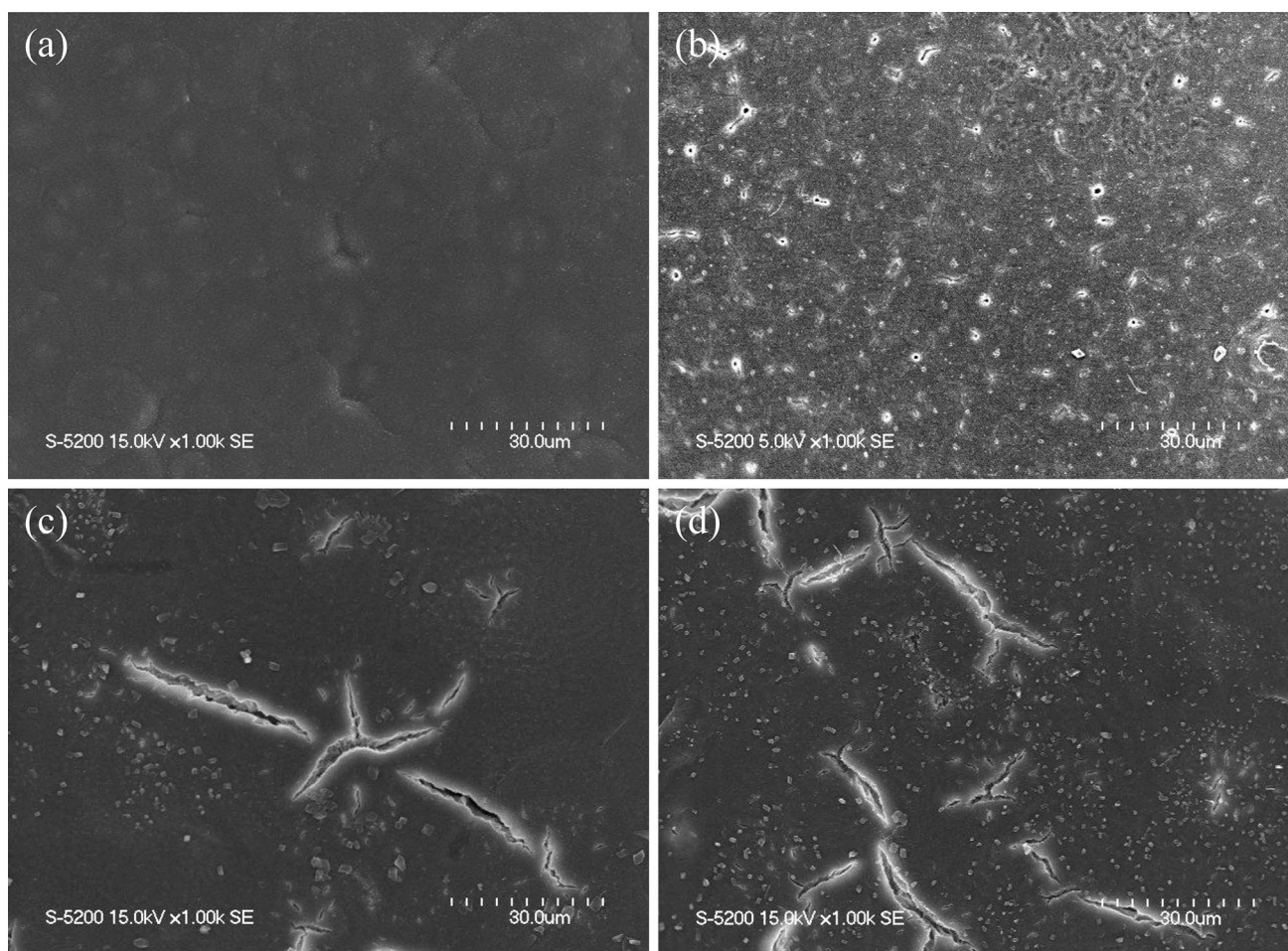


Fig. 9 SEM images of the PDO100/CS0 blend with respect to the degradation time: **a** 0 w, **b** 4 w, **c** 8 w, and **d** 12 w

in the remaining segments. However, when the hydrolysis progressed further, the crystalline regions were attacked as well. As a result, the crystallinity of PDO first increased and then decreased after 8 weeks. In the case of the pure PDO, the melting temperature (T_m) and enthalpy of melting (ΔH_m) were 110.3 °C and 66.1 °C, respectively.

As can be seen from Table 2, the melting temperatures of the PDO/chitosan was affected by the relatively low melt viscosity of chitosan. Specifically, T_m and ΔH_m in the blends decreased as the chitosan content increased. This implied that the presence of chitosan led to a decrease in the crystallinity of PDO since the movement of the polymer segments was impeded by chitosan [34].

Figure 9 shows the SEM images of the pure PDO film with respect to the degradation time. The sample surface was smooth at the beginning (0 w), but small holes were

observed on the surface during the hydrolysis. After the eighth week of hydrolysis (Fig. 9c), the cracks appeared on the surface, which allow water to penetrate the matrix. These cracks became more and deeper over time and eventually were connected. In other words, the chain loss happens as time elapses.

The SEM images shown in Fig. 10a confirmed that there was no phase separation in the blend, which implies a good miscibility of the blend. This result is in agreement with the DSC result. For the hydrolysis, the PDO film with 30 wt% chitosan did not show defects on the surface until 4 weeks (Fig. 10). The surface was not smooth, and deformation occurred in the 8th week sample (Fig. 10c). Also, some holes and empty spaces were formed due to the swelling of chitosan powders [35].

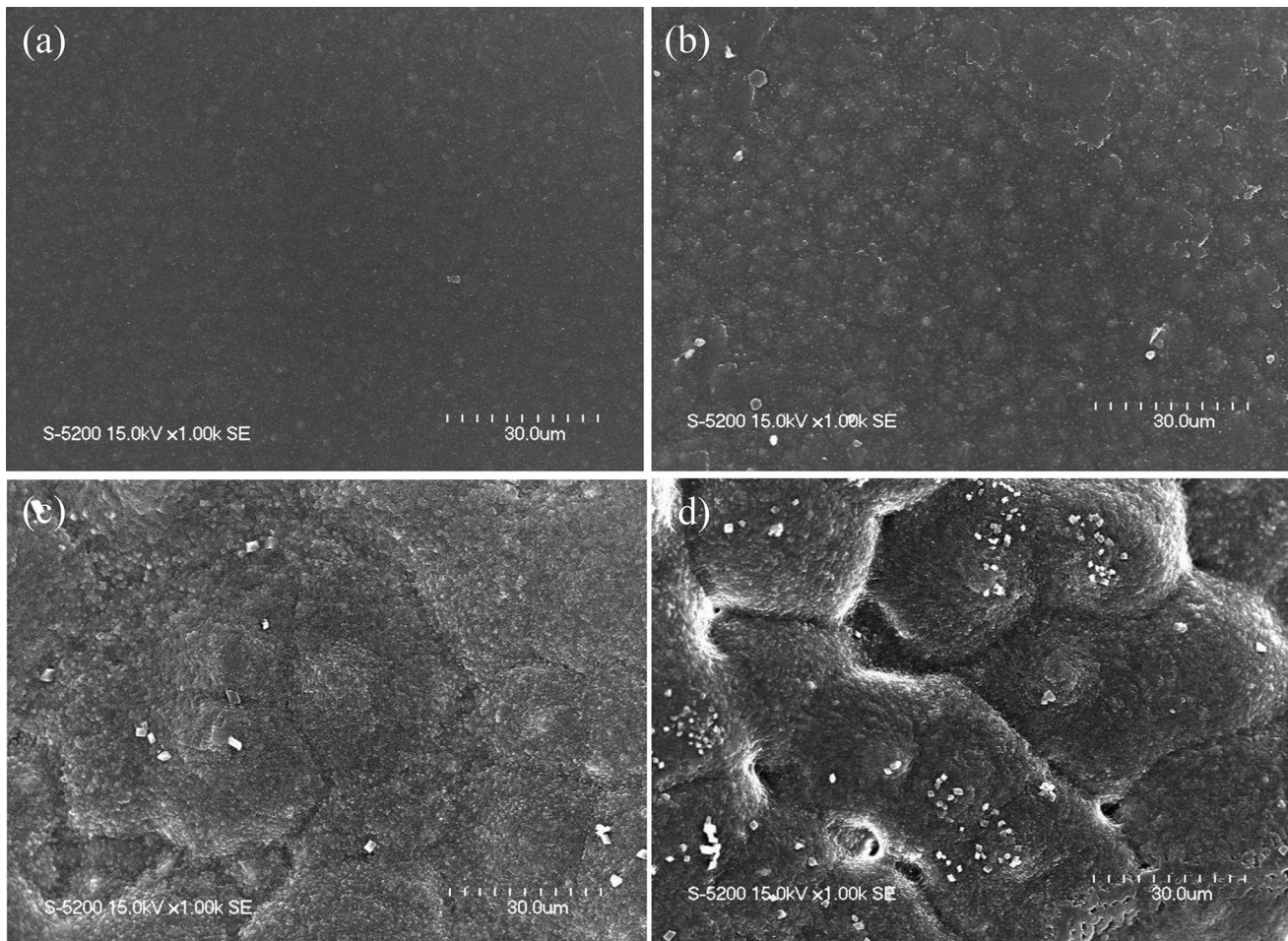


Fig. 10 SEM images of the PDO70/CS30 blend with respect to the degradation time: **a** 0 w, **b** 4 w, **c** 8 w, and **d** 12 w

Conclusions

In this study, the biodegradable PDO/chitosan films were prepared via the film casting. The thermal and mechanical properties of the blends were evaluated through DMA, TGA, DSC, and UTM analyses. Also, the miscibility of the blend was investigated experimentally. The FTIR and NMR results showed that the intermolecular hydrogen bonds exist between chitosan and PDO. In addition, the biodegradability of the sample was tested for 12 weeks in the PBS solution. It was found that chitosan plays an important role in enhancing the mechanical properties of the blend films. The chitosan embedded film showed significantly different thermal properties and morphologies from the pure PDO film. We conclude that physicochemical properties of PDO film can be controlled by blending with chitosan for biomedical applications such as GBR.

Acknowledgements This work was supported by the GRRC program of Gyeonggi Province (GRRC Dankook 2016–B03). In addition, this research was supported by the Basic Science Research Program

through the National Research Foundation of Korea (NRF), funded by the Ministry of Education (2018R1A5A1024127).

Declarations

Conflict of interest The authors declare no conflicts of financial or non-financial competing interest.

References

1. Di Raimondo R, Sanz-Esporrín J, Sanz-Martin I, Plá R, Luengo F, Vignoletti F, Nuñez J, Sanz M (2021) Hard and soft tissue changes after guided bone regeneration using two different barrier membranes: an experimental in vivo investigation. *Clin Oral Investig* 25(4):2213–2227
2. Guo H, Xia D, Zheng Y, Zhu Y, Liu Y, Zhou Y (2020) A pure zinc membrane with degradability and osteogenesis promotion for guided bone regeneration: in vitro and in vivo studies. *Acta Biomater* 106:396–409
3. Greenstein G, Greenstein B, Cavallaro J, Tarnow D (2009) The role of bone decortication in enhancing the results of guided bone regeneration: a literature review. *J Periodontol* 80(2):175–189

4. Gentile P, Chiono V, Tonda-Turo C, Ferreira AM, Ciardelli G (2011) Polymeric membranes for guided bone regeneration. *Biotechnol J* 6(10):1187–1197
5. Elgali I, Omar O, Dahlin C, Thomsen P (2017) Guided bone regeneration: materials and biological mechanisms revisited. *Eur J Oral Sci* 125(5):315–337
6. Jung RE, Fenner N, Hämmerle CH, Zitzmann NU (2013) Long-term outcome of implants placed with guided bone regeneration (GBR) using resorbable and non-resorbable membranes after 12–14 years. *Clin Oral Implants Res* 24(10):1065–1073
7. Peng W, Chen JX, Shan XF, Wang YC, He F, Wang XJ, Tan LL, Yang K (2019) Mg-based absorbable membrane for guided bone regeneration (GBR): a pilot study. *Rare Met* 38(6):577–587
8. Zhang L, Xiong C, Deng X (1995) Biodegradable polyester blends for biomedical application. *J Appl Polym Sci* 56(1):103–112
9. John J, Mani R, Bhattacharya M (2002) Evaluation of compatibility and properties of biodegradable polyester blends. *J Polym Sci Part A: Polym Chem* 40(12):2003–2014
10. Sabino MA, González S, Márquez L, Feijoo JL (2000) Study of the hydrolytic degradation of polydioxanone PPDx. *Polym Degradation Stab* 69(2):209–216
11. Bai W, Zhang LF, Li Q, Chen DL, Xiong CD (2010) In vitro hydrolytic degradation of poly (para-dioxanone)/poly (D, L-lactide) blends. *Mater Chem Phys* 122(1):79–86
12. Ebrahimpour M, Safekordi AA, Mousavi SM, Heydarinasab A (2018) A miscibility study on biodegradable poly butylene succinate/polydioxanone blends. *J Polym Res* 25(2):35
13. Ikejima T, Inoue Y (2000) Crystallization behavior and environmental biodegradability of the blend films of poly (3-hydroxybutyric acid) with chitin and chitosan. *Carbohydr Polym* 41(4):351–356
14. Kumar MNVR, Muzzarelli RAA, Muzzarelli C, Sashiwa H, Domb AJ (2004) Chitosan chemistry and pharmaceutical perspectives. *Chem Rev* 104(12):6017–6084
15. Chandy T, Sharma CP (1990) Chitosan-as a biomaterial. *Biomater Artif Cells Artif Organs* 18(1):1–24
16. Wan Y, Wu H, Yu A, Wen D (2006) Biodegradable polylactide/chitosan blend membranes. *Biomacromol* 7(4):1362–1372
17. Shih CM, Shieh YT, Twu YK (2009) Preparation and characterization of cellulose/chitosan blend films. *Carbohydr Polym* 78(1):169–174
18. Tamimi M, Rajabi S, Pezeshki-Modaress M (2020) Cardiac ECM/chitosan/alginate ternary scaffolds for cardiac tissue engineering application. *Int J Biol Macromol* 164:389–402
19. Ishikiriyama K, Pyda M, Zhang G, Forschner T, Grebowicz J, Wunderlich B (1998) Heat capacity of poly-p-dioxanone. *J Macromol Sci B* 37(1):27–44
20. Lustriane C, Dwivany FM, Suendo V, Reza M (2018) Effect of chitosan and chitosan-nanoparticles on post harvest quality of banana fruits. *J Plant Biotechnol* 45(1):36–44
21. Kapantaidakis G, Kaldis S, Dabou X, Sakellaropoulos G (1996) Gas permeation through PSF-PI miscible blend membranes. *J Membr Sci* 110(2):239–247
22. Piotrowska-Kirschling A, Brzeska J (2020) The effect of chitosan on the chemical structure, morphology, and selected properties of polyurethane/chitosan composites. *Polymers* 12(5):1205
23. Younes I, Hajji S, Frachet V, Rinaudo M, Jellouli K, Nasri M (2014) Chitin extraction from shrimp shell using enzymatic treatment. Antitumor, antioxidant and antimicrobial activities of chitosan. *Int J Biol Macromol* 69:489–498
24. Ikejima T, Yagi K, Inoue Y (1999) Thermal properties and crystallization behavior of poly (3-hydroxybutyric acid) in blends with chitin and chitosan. *Macromol Chem Phys* 200(2):413–421
25. Gartner C, López BL, Sierra L, Graf R, Spiess HW, Gaborieau M (2011) Interplay between structure and dynamics in chitosan films investigated with solid-state NMR, dynamic mechanical analysis, and X-ray diffraction. *Biomacromol* 12(4):1380–1386
26. Masson JF, Manley RSJ (1991) Cellulose/poly (4-vinylpyridine) blends. *Macromolecules* 24(22):5914–5921
27. Katcha SW, Flintsch GW (2012) Fractional viscoelastic models: master curve construction, interconversion, and numerical approximation. *Rheol Acta* 51(8):675–689
28. Abay AK, Gebeyehu MB, Lin HK, Lin PC, Lee JY, Wu CM, Murakami RI, Chiang TC (2016) Preparation and characterization of poly (lactic acid)/recycled polypropylene blends with and without the coupling agent, n-(6-aminohexyl) aminomethyltriethoxysilane. *J Polym Res* 23(9):198
29. Diab MA, El-Sonbati AZ, Bader DMD, Zoromba MS (2012) Thermal stability and degradation of chitosan modified by acetophenone. *J Polym Environ* 20(1):29–36
30. Han CM, Lih E, Choi SK, Bedair TM, Lee YJ, Park W, Han DK, Son JS, Joung YK (2018) Biodegradable sheath-core biphasic monofilament braided stent for bio-functional treatment of esophageal strictures. *J Ind Eng Chem* 67:396–406
31. Sharmin N, Khan RA, Salmieri S, Dussault D, Lacroix M (2012) Fabrication and characterization of biodegradable composite films made of using poly (caprolactone) reinforced with chitosan. *J Polym Environ* 20(3):698–705
32. Correlo V, Boesel L, Bhattacharya M, Mano J, Neves N, Reis R (2005) Properties of melt processed chitosan and aliphatic polyester blends. *Mater Sci Eng* 403(1–2):57–68
33. Böstman O (1991) Absorbable implants for the fixation of fractures. *J Bone Joint Surg* 73(1):148–153
34. Wu CS (2005) A comparison of the structure, thermal properties, and biodegradability of polycaprolactone/chitosan and acrylic acid grafted polycaprolactone/chitosan. *Polymer* 46(1):147–155
35. Torres-Huerta AM, Palma-Ramírez D, Dominguez-Crespo MA, Del Angel-López D, De La Fuente D (2014) Comparative assessment of miscibility and degradability on PET/PLA and PET/chitosan blends. *Eur Polym J* 61:285–299

Publisher's Note Springer Nature remains neutral with regard to jurisdictional claims in published maps and institutional affiliations.